THERMAL PROTECTION SYSTEMS MANNED SPACECRAFT FLIGHT EXPERIENCE

Donald M. Curry
NASA/Johnson Space Center
Houston, Texas

INTRODUCTION

Since the first U. S. manned entry, Mercury (May 5, 1961), seventy-five manned entries (figs. 1, 2) have been made resulting in significant progress in the understanding and development of Thermal Protection Systems (TPS) for manned rated spacecraft. Figures 3 and 4 compare the TPS materials and systems installed on these spacecraft. The first three vehicles (Mercury, Gemini, Apollo) used ablative (single-use systems) while the Space Shuttle Orbiter TPS is a multimission system. A TPS figure of merit, unit weight lb/ft^2, illustrates the advances in TPS material performance from Mercury (10.2 lb/ft^2) to the Space Shuttle (1.7 lb/ft^2).

Vehicle	No. of Entries
Orbital Return	
Mercury (1961-63)	6
Gemini (1965-66)	10
Apollo (1968-75)	5
Shuttle (Thru Feb., 1992)	44
Lunar Return	
Apollo (1969-72)	10

Figure 1. U.S. manned spacecraft.

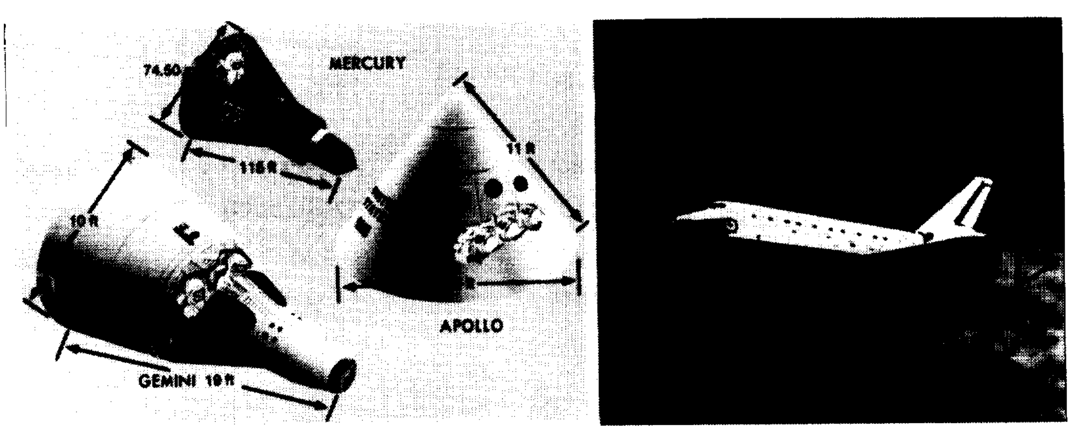

Figure 2. Manned spacecraft entry vehicles.

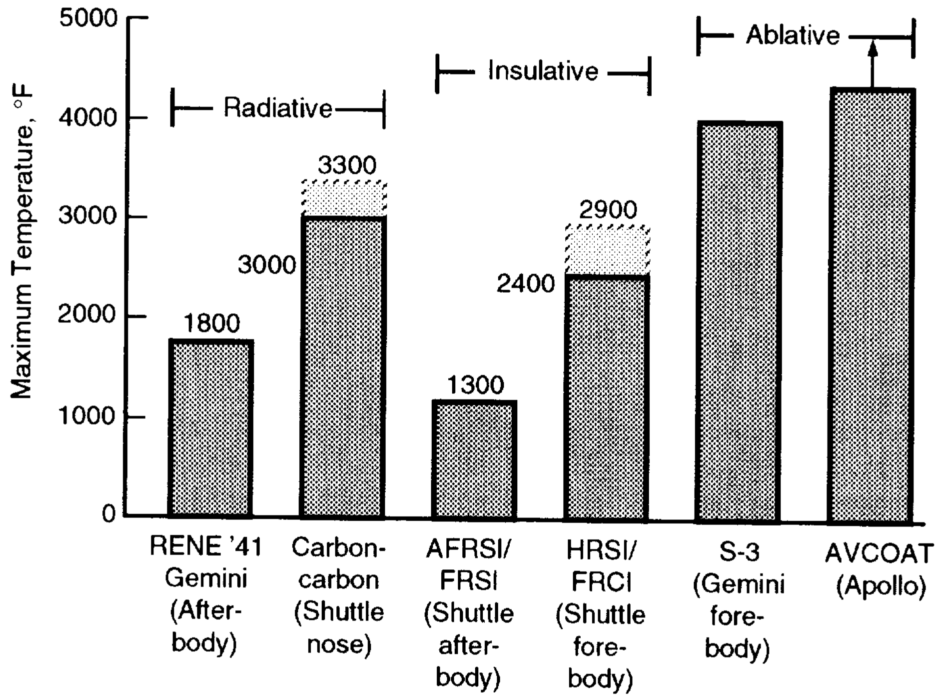

Figure 3. Manned spacecraft thermal protection materials.

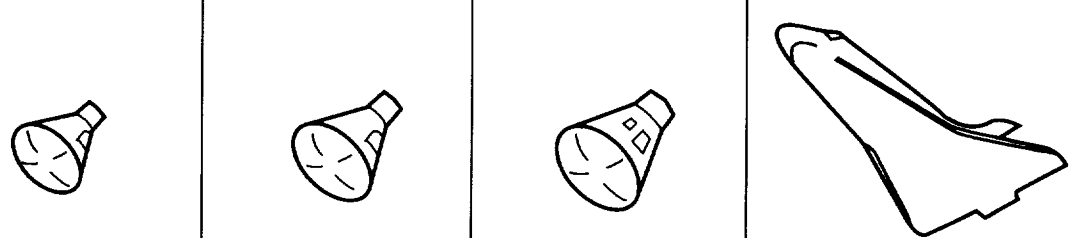

	Mercury	Gemini	Apollo	Shuttle
Area	32 ft^2	45 ft^2	365 ft^2	11 895 ft^2
Weight	315 lb	348 lb	1465 lb	18 904 lb
Wt/ft^2	10.2	7.5	3.9	1.7
Material	Ablator (Fiberglass-phenolic)	Ablator (Corning DC 235)	Ablator (AVCO 5026-39)	Rigidized silica fibers
Density	114 lb/ft^3	54 lb/ft^3	32 lb/ft^3	9-22 lb/ft^3
Usage	1 flight	1 flight	1 flight	100 flights

X101442M

Figure 4. Manned spacecraft entry TPS.

In the design of a passive TPS for atmospheric entries, ablative materials have provided a number of inherent advantages in both thermal performance and structural-mechanical properties. Ablative materials were successfully used for both Earth-orbital (Mercury, Gemini) and lunar return (Apollo) velocities. The Apollo TPS material (AVCO 5026-39 HCG) was characterized using both ground tests (plasma jet and radiant) and unmanned flight tests (earth-orbital/lunar return). Design of this TPS was accomplished using two trajectories; maximum heat rate (~700 BTU/ft^2-sec) for surface temperature/recession and heat load (~44,000 BTU/ft^2) for structural temperature. The conservatively designed TPS thickness, measured surface recession and char thickness, for a typical Apollo-lunar return is illustrated in figure 5.

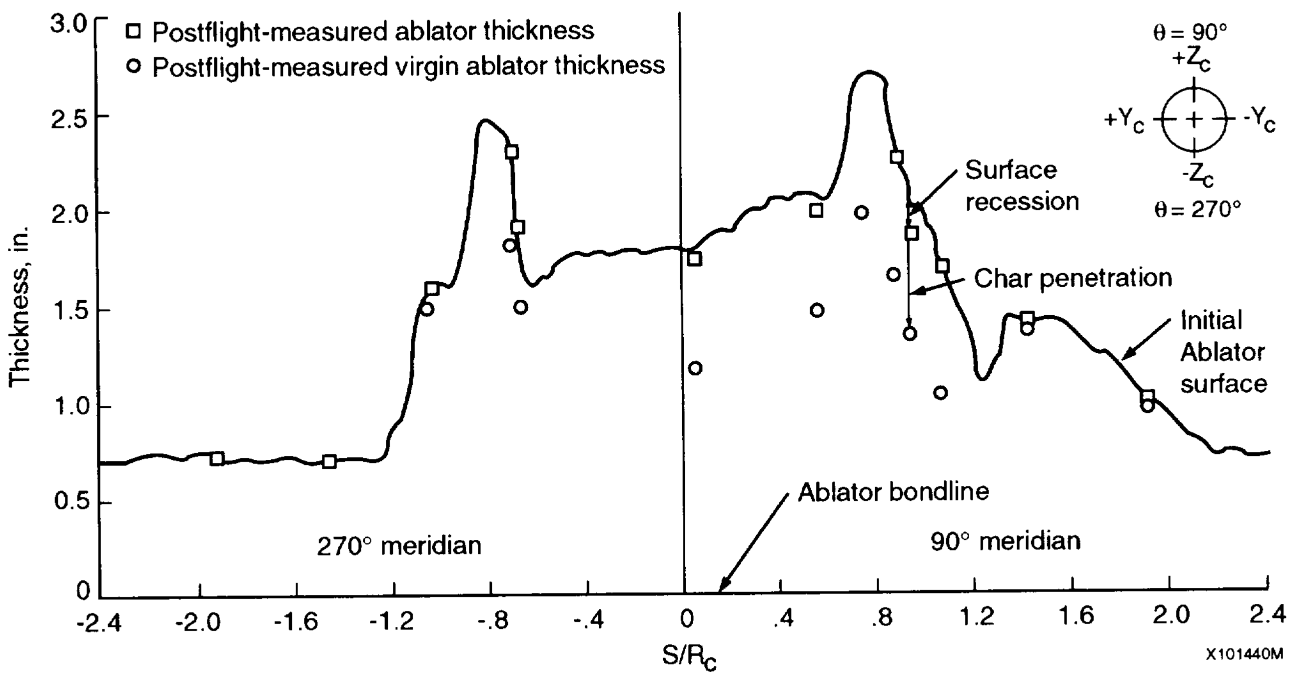

Figure 5. Comparisons of measured ablator thermal performance.

Prior to the Space Shuttle program, all manned space vehicles used ablator materials having a one-mission capability. In contrast, the Space Shuttle Orbiter TPS had to be reusable to minimize costs and minimum weight to meet vehicle requirements. The Orbiter TPS design, in contrast to previous spacecraft, was verified with flight data from the first five manned flights of the Orbiter Columbia. A comparison of the design and flight environments for the Space Shuttle Orbiter is shown in figure 6. The Orbiter flight parameters, in particular the 40° angle of attack, allowed relatively lower reference total heat load and heating rate than was predicted for the design trajectory.

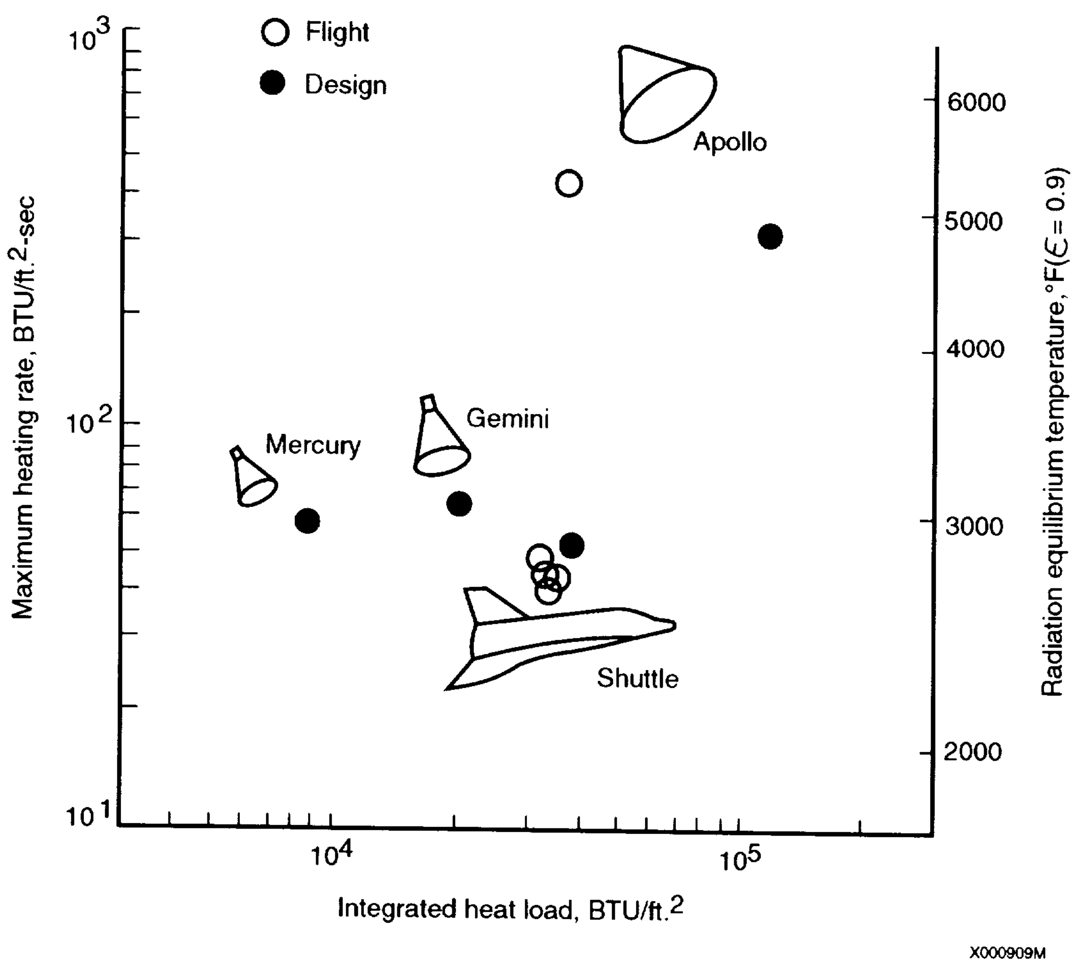

Figure 6. TPS design and flight test environments.

ORBITER TPS MATERIALS

The Orbiter TPS (fig. 7) consists basically of two material systems, reusable surface insulation (RSI) and reinforced carbon-carbon (RCC). The RSI-TPS is further characterized by three rigid ceramic insulation materials:

- high temperature reusable surface insulation (HRSI) consisting of black-coated LI-900/ LI2200 coated tiles,
- low temperature reusable surface insulation (LRSI) consisting of white-coated LI-900 tiles,
- fibrous refractory composite insulation (FRCI-12) with black coating

And two flexible insulation materials:

- flexible reusable surface insulation (FRSI)
- advanced flexible reusable surface insulation (AFRSI).

The rigidized ceramic material is used over the major portion of the Orbiter for temperatures ranging from 1300 to 2300°F. The upper surface areas, where temperatures are generally less than 1300°F, the flexible insulation materials are used. The RCC is used for those areas (i.e., nose cap, wing leading edge) where temperatures exceed 2300°F. Material distribution (peak temperature) and thickness determination (heat load) were selected to minimize weight while retaining a multi-mission capability. AFRSI and FRCI were not part of the original TPS design, AFRSI was first flown on STS-6 (OV-099) and FRCI on the fourth flight of OV-099 (41B).

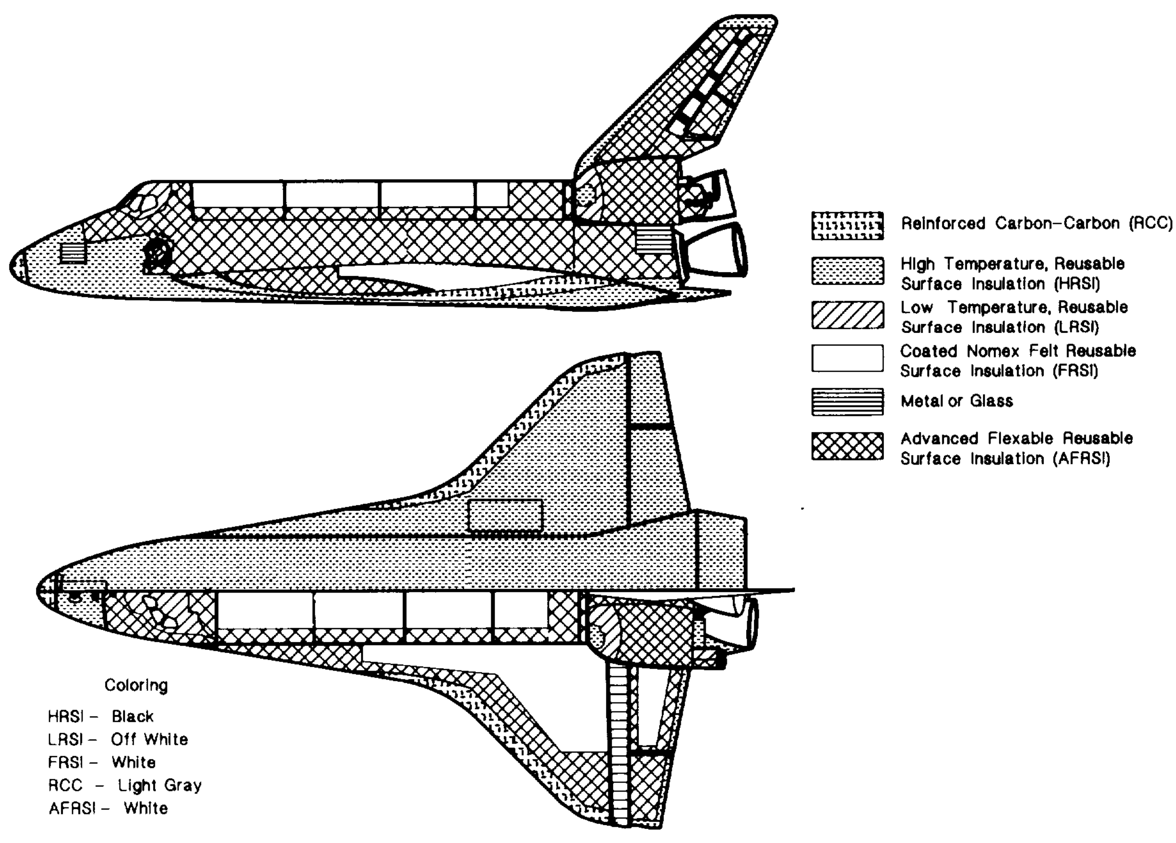

Figure 7. Thermal protection system, Orbiter 103 and subsequent orbiters.

ORBITER TPS PEAK SURFACE TEMPERATURE

A limited number of surface temperature measurements have been made for the various Orbiter flights. Figure 8 presents some typical results. These surface temperature measurements are used in the identification of any anomalies during the entry (i.e., gap/step heating, transition effects). These temperatures are also used to indicate changes in the surface condition of the RSI tiles (i.e., surface catalysis, emissivity).

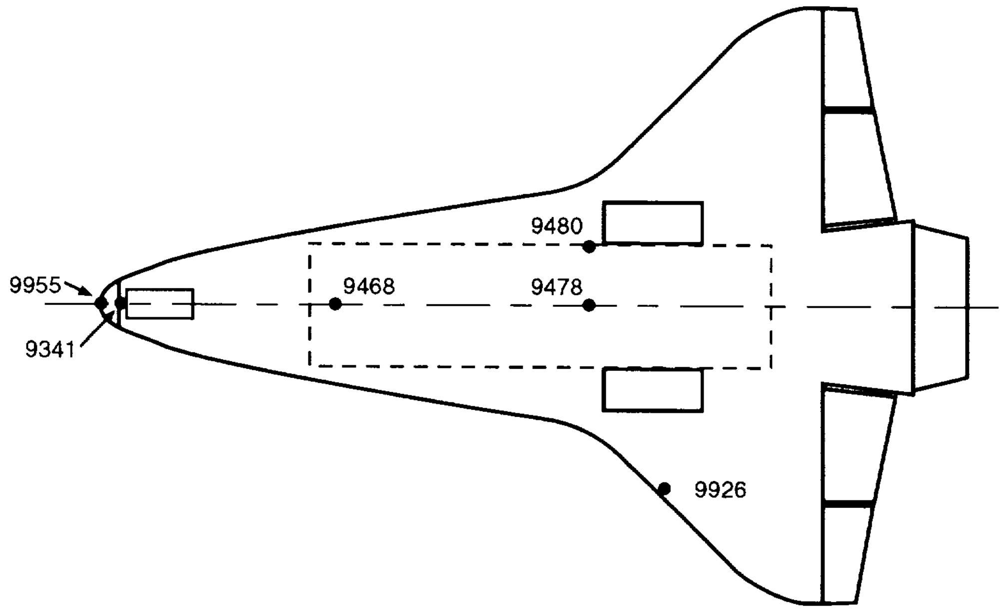

Flight	Vehicle	VO7T-9468	VO7T-9478	VO7T-9480	VO9T-9341	VO9T-9955	VO9T-9926
STS-1	OV-102	-	-	-	-	-	-
STS-2	OV-102	1530	1560	1500	2080	-	2470**
STS-3	OV-102	2035*	1470	1460	-	-	2460**
STS-4	OV-102	-	-	-	-	-	-
STS-5	OV-102	1750*	1600*	1400	2160	2605**	2501**
STS-26	OV-103	1505	-	1465	-	-	-
STS-27	OV-104	-	1600	1600	-	-	-
STS-29	OV-103	-	-	-	-	-	-
STS-30	OV-104	-	1435	1400	-	-	-
STS-28	OV-102	1350	1750	1790	-	-	-
STS-34	OV-104	-	1440	1470	-	-	-
STS-33	OV-103	1560	-	1490	-	-	-
STS-32	OV-102	1390	1380	1400	-	-	-
STS-36	OV-104	-	1450	1340	-	-	-
STS-31	OV-103	1590	-	1480	-	-	-
STS-41	OV-103	-	-	1500	-	-	-
STS-38	OV-104	-	1410	1300	-	-	-
STS-35	OV-102	-	-	-	-	-	-
STS-37	OV-104	-	1400	1310	-	-	-
STS-39	OV-103	1420	-	1460	-	-	-
STS-40	OV-102	1430	1520	1500	-	-	-
STS-43	OV-104	-	1390	-	-	-	-
STS-48	OV-103	1620	-	1700	-	-	-
STS-44	OV-104	-			-	-	-

* Catalytic coated tile
** RCC Inner Surface

X101438M

Figure 8. Orbiter peak surface temperatures.

ORBITER PEAK STRUCTURAL TEMPERATURE

The RSI performs the required thermal protection function during entry by two primary means of heat dissipation. A large percentage (~95 percent) of the heat energy is reradiated to the atmosphere and the remaining heat energy is effectively retarded by the low diffusivity of the basic insulation material. The basic thermal performance of the RSI can be evaluated by three important parameters: the induced surface temperature profile, the transient response of the RSI interior, and the structural temperature response. Figure 9 shows a typical distribution of STS flight measure peak structural temperatures. Since the Orbiter flight envelope and the design trajectory are relatively equal (heat rate/heat load); these low structural temperatures (350° design) provide a positive thermal margin. As with surface temperature, these structural temperatures can be used to indicate any potential degradation in RSI material with reuse.

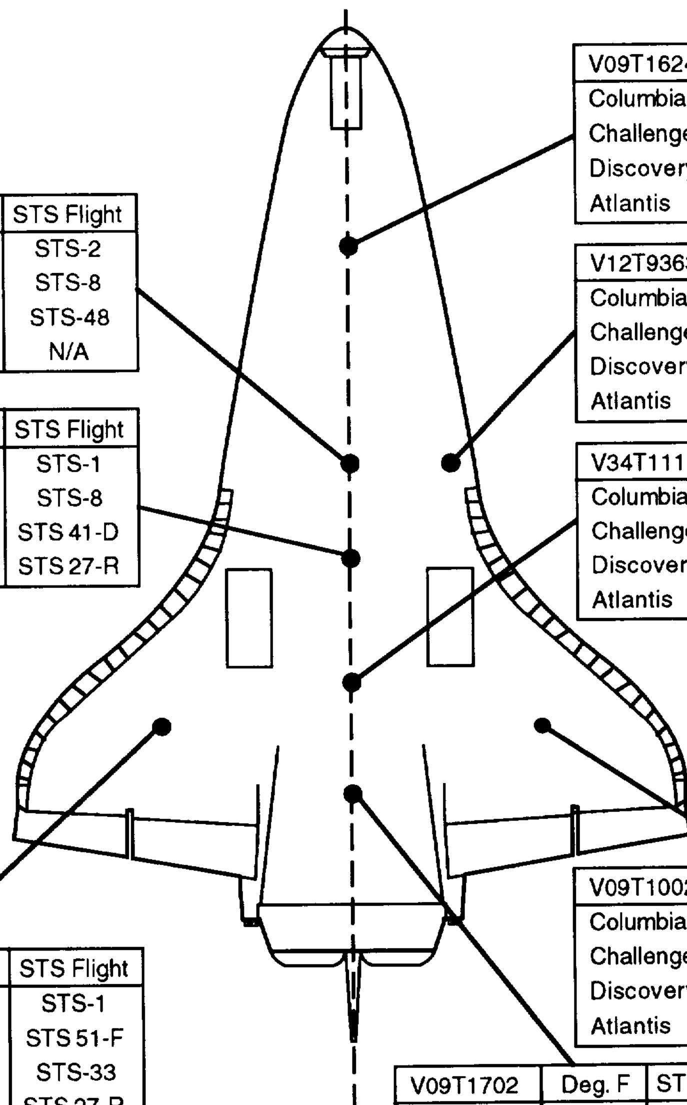

V09T1624	Deg. F	STS Flight
Columbia	153	STS-1
Challenger	153	STS-8
Discovery	156	STS-48
Atlantis	175	STS 27-R

V34T9892	Deg. F	STS Flight
Columbia	187	STS-2
Challenger	210	STS-8
Discovery	197	STS-48
Atlantis	N/A	N/A

V12T9363	Deg. F	STS Flight
Columbia	160	STS-2
Challenger	143	STS-8
Discovery	152	STS 41-D
Atlantis	N/A	N/A

V34T1110	Deg. F	STS Flight
Columbia	196	STS-1
Challenger	191	STS-8
Discovery	170	STS 41-D
Atlantis	188	STS 27-R

V34T1112	Deg. F	STS Flight
Columbia	225	STS 28-R
Challenger	203	STS-8
Discovery	202	STS-48
Atlantis	207	STS 27-R

V09T1000	Deg. F	STS Flight
Columbia	153	STS-1
Challenger	146	STS 51-F
Discovery	130	STS-33
Atlantis	164	STS 27-R

V09T1002	Deg. F	STS Flight
Columbia	161	STS-9
Challenger	143	STS 41-G
Discovery	138	STS-48
Atlantis	146	STS-27R

V09T1702	Deg. F	STS Flight
Columbia	206	STS 28-R
Challenger	193	STS-8
Discovery	204	STS-48
Atlantis	209	STS 27-R

X101439M

Figure 9. Orbiter maximum structure temperatures.

ORBITER TPS FLIGHT EXPERIENCE
AERODYNAMIC FLOW DAMAGE

The RSI system thermal/structural integrity for the most part has been excellent for all STS flights. The major areas of TPS requiring repair/refurbishment, replacement and/or design change have involved impact damage, gap filler degradation, gas heating in joint regions, seal performance, and penetrations and prevention of hot gas radiation leaks. An example of aerodynamic flow damage occurred on STS-6. The leading edge area of the orbital maneuvering system (OMS) pod was covered with AFRSI material. As can be seen in figure 10a, the AFRSI sustained severe damage from loss of the outer fabric to complete removal of thermal insulation. Postflight and laboratory investigations indicated no evidence of thermal degradation, therefore, the damage was attributed primarily to mechanical loading of the AFRSI blankets due to aerodynamic flow forces. This area was subsequently redesigned using rigid ceramic tiles (fig. 10b).

Right-hand OMS POD, STS-6 Left-hand OMS POD, STS-6

Figure 10a. OMS POD-AFRSI damage.

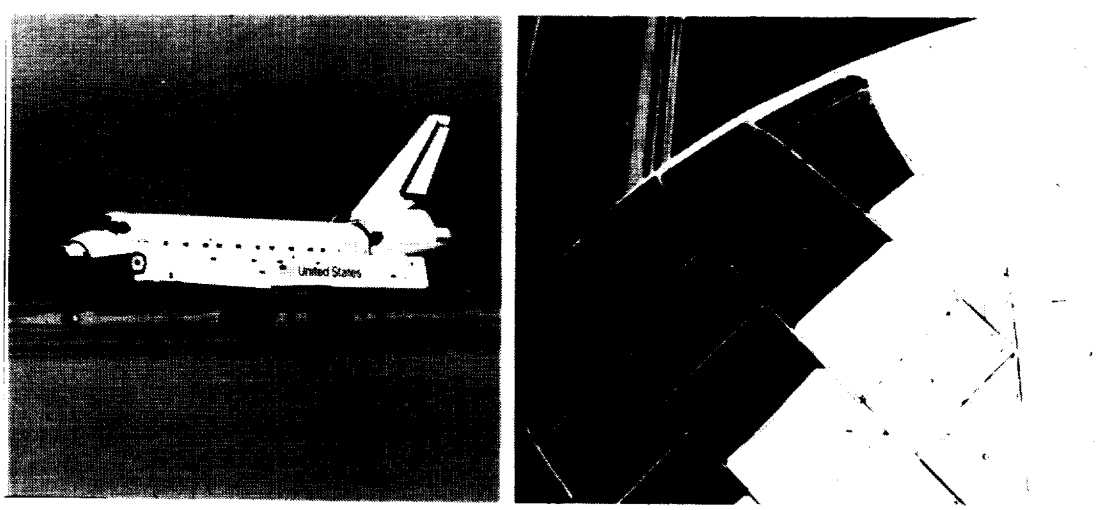

Figure 10b. OMS-POD tile redesign.

ORBITER TPS FLIGHT EXPERIENCE
RSI TILE IMPACT DAMAGE

While the Orbiter is in the launch configuration, the TPS is not protected from the natural environment (i.e., rain, hail, etc.) Likewise, during the launch phase, on-orbit and landing phases, as well as the ferry flight configuration; the Orbiter TPS is exposed to damage from ice, foreign objects, debris, etc. An example of debris impact damage on the lower surface of the wing is shown in figure 11. The reaction curved glass (RCG) coating has been lost as a result of the impact exposing the basic silica material. Depending on the size and depth of the damage, a series of repairs have been developed to return the tile to full service.

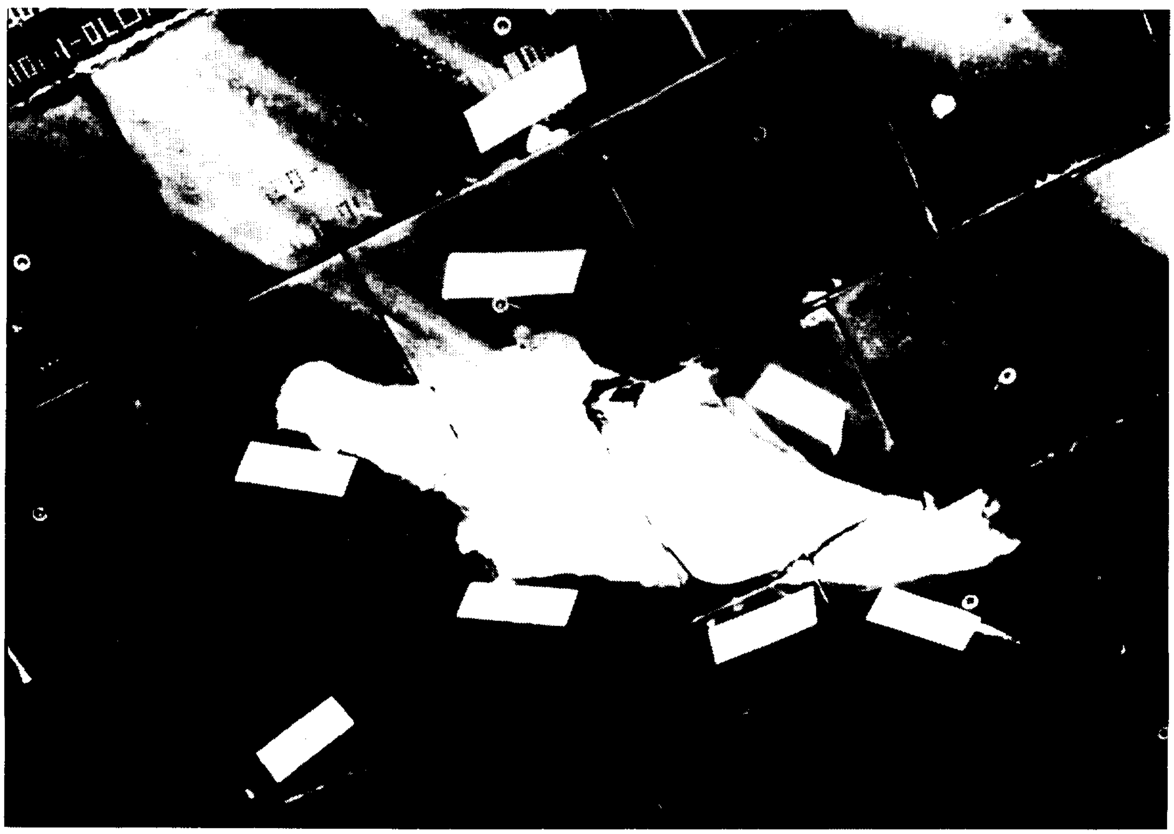

Figure 11. Wing debris impact gouge.

ORBITER TPS FLIGHT EXPERIENCE
RSI TILE IMPACT DAMAGE

For the most part, tile damage due to rain, hail or debris impact has not resulted in tile loss. STS-27 (OV-104) was an example of complete tile removal due to a combination of impact and reentry thermal exposure (fig. 12). The loss of tile occurred prior to entry (probably during launch) as evidenced by thermal degradation of strain isolation pad (SIP) and filler bar; however, no structural burn-thru occurred. The structure was refurbished and new tiles installed.

Figure 12. Lower forward chine missing tile.

ORBITER TPS FLIGHT EXPERIENCE
GAP FILLER DAMAGE

Fabric/ceramic gap fillers and flow stoppers are used extensively between tiles, TPS penetrations, RCC/RSI interfaces, and moveable interfaces. Gap fillers fabricated from quartz and Nextel become brittle and breach with continued reuse and cycling at temperatures in excess of 2000°F. Significant handling damage occurs once the gap filler is brittle. Gap filler shrinkage between tiles results in higher tile temperature (due to gap/step heating) and subsequent localized tile shrinkage/melting. An example of gap filler breaching and tile slumping is shown in figure 13. The use of a ceramic (colloidal silica) coating (designated C-9) significantly enhances the performance of the gap filler surface. C-9 coated gap fillers (Nextel and quartz) have successfully survived arc testing to 2500°F and are now installed in the Orbiter fleet. C-9 coating also has been applied to rigidize the AFRSI blankets and provide additional resistance to handling and impact damage.

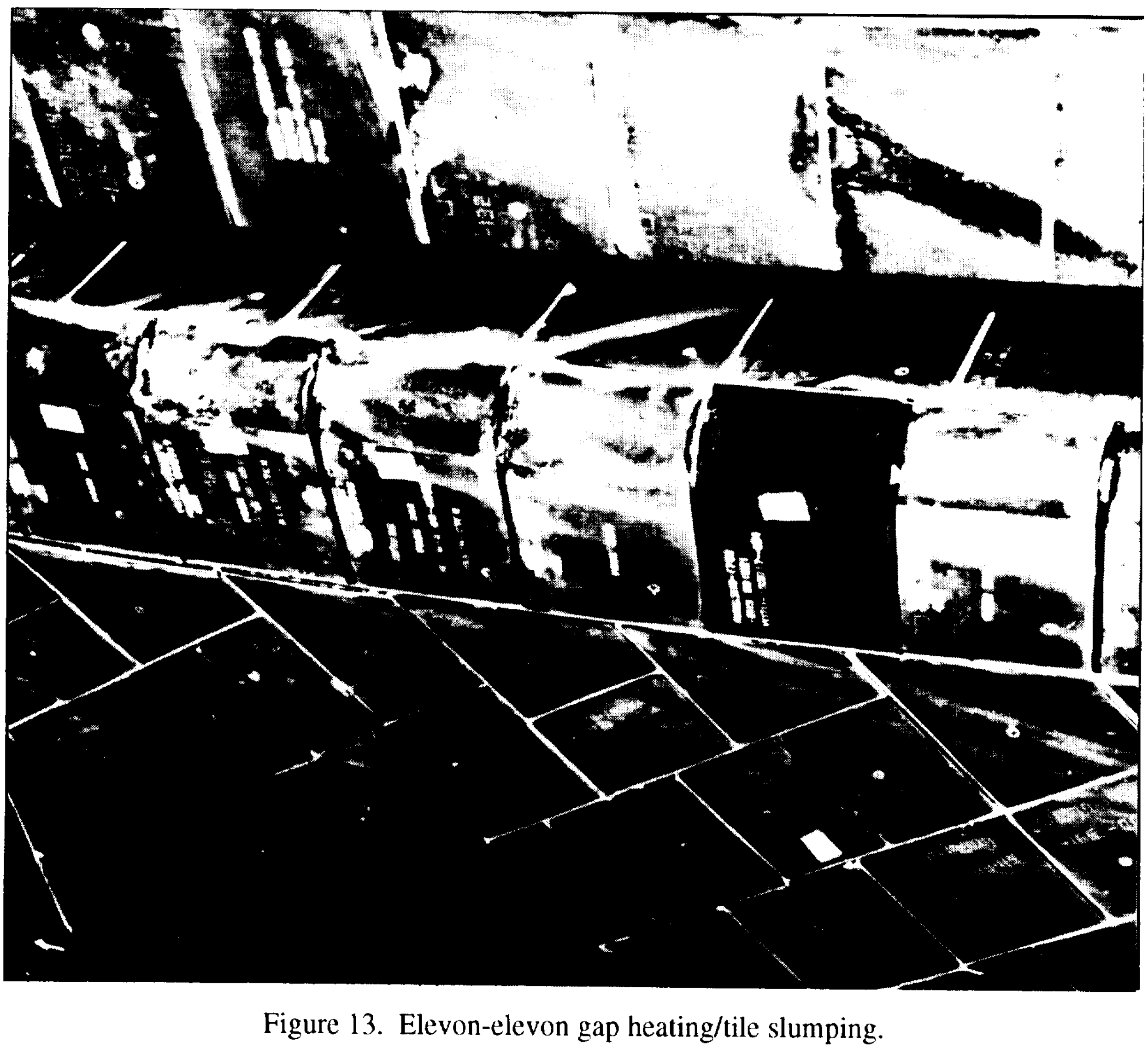

Figure 13. Elevon-elevon gap heating/tile slumping.

ORBITER TPS FLIGHT EXPERIENCE
ELEVON LEADING EDGE

All three Orbiter vehicles have experienced TPS damage, over temperature of the elevon leading edge carrier plates,and primary seal holder. This damage has consisted of gas filler breaches, tile slumping, tile failure,and structure melting. The basic nature of the elevon leading edge/cove geometry (fig. 14a) creates pressure and heating gradients within the tile installation. This increased heating and pressure results in degradation of the gap fillers along the entire span. Potential leak sources (seal, gap filler, carrier plate, Columbia seal) also increase degradation of the gap filler.

Once the gas filler degrades, slumping on adjacent and downstream tiles occurs resulting in hot gas flow into the elevon seal/cove area. The worst damage was experienced on STS-51D (OV-103), where significant melting occurred on the aluminum carrier panel (Fig. 14b). This damage was worst than had been experienced on previous Orbiter flights and is generally attributed to more negative elevon deflection and higher surface roughness. Elimination of leak paths and reduction of the wing elevon roughness has been implemented to minimize elevon leading edge damage.

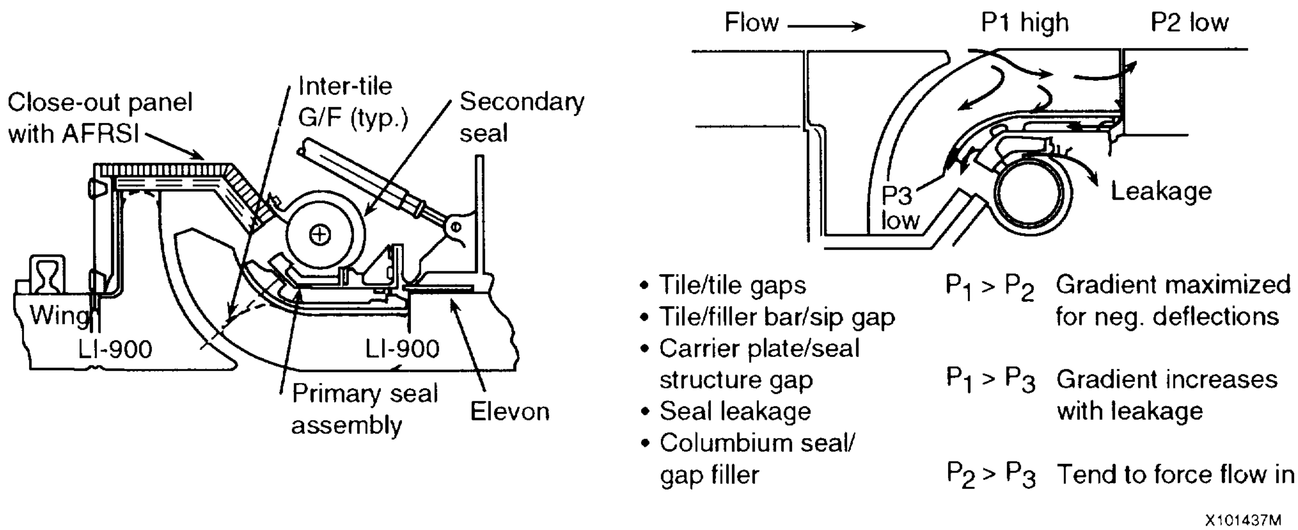

Figure 14a. Elevon leading edge design components and flow paths.

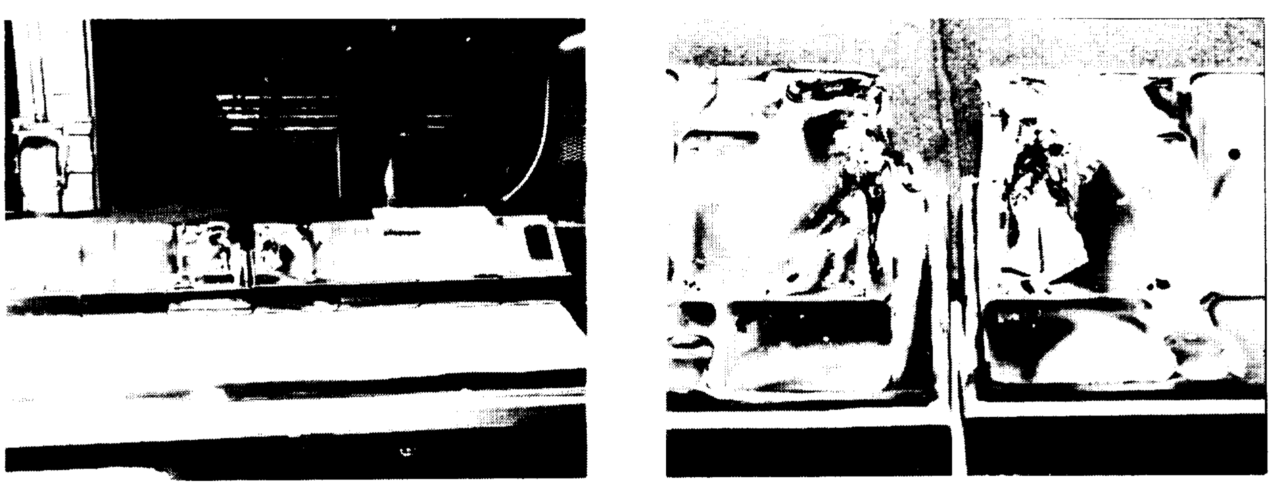

Figure 14b. Elevon cove carrier panel damage.

ORBITER TPS FLIGHT EXPERIENCE
NOSE GAP LOWER SURFACE INTERFACE TILE DAMAGE

Damage to the nose cap lower windward surface interface tiles (slumping of tiles along tile outer edge) forward of the nose gear door has occurred on several STS flights. The most significant damage occurred on STS-5 when hot gas penetration into the gap between two interface tiles caused slumping/melting of the tiles; thermal damage to the gap fillers, filler bars, and flow stoppers; and local melting of the aluminum carrier plate (fig. 15).

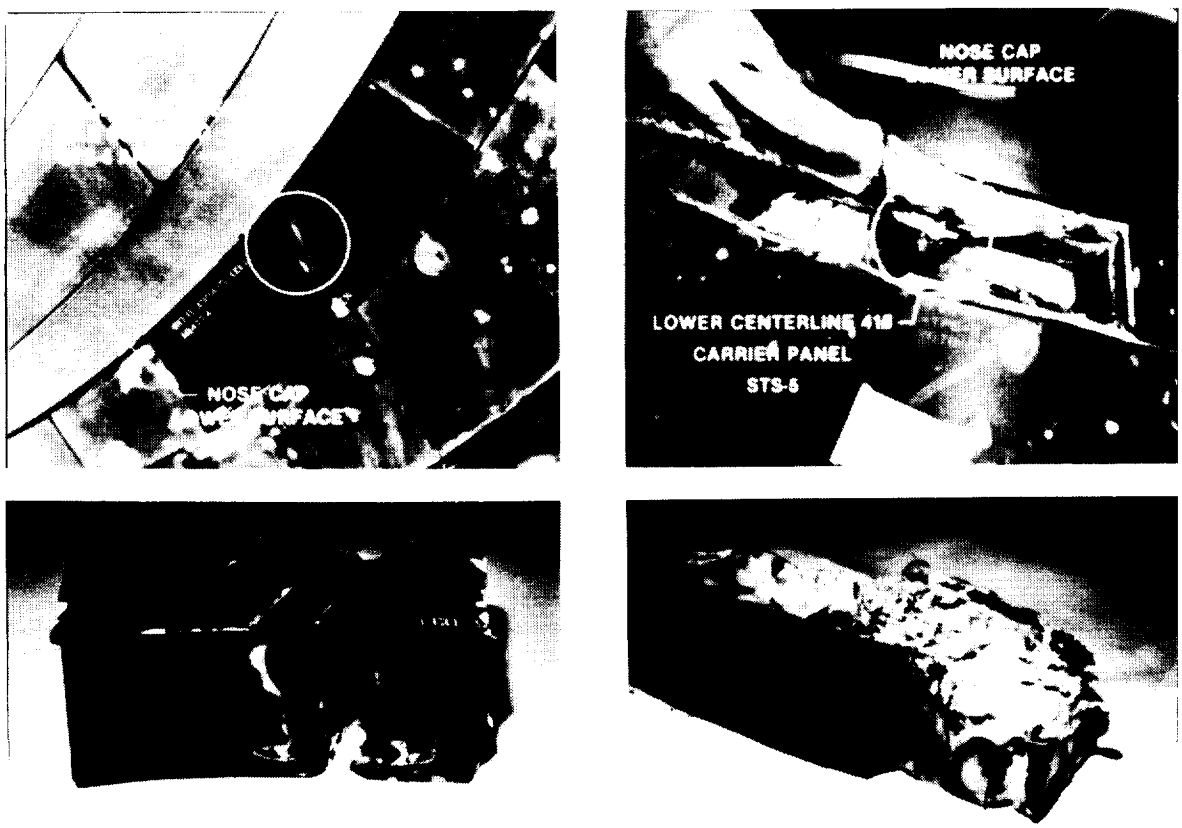

Figure 15. Nose cap lower surface interface tile damage - STS-5.

ORBITER TPS FLIGHT EXPERIENCE
RCC CHIN PANEL

The RSI tiles installed between the nose gap and the nose landing gear doors have been vulnerable to external tank debris impact damage and have experienced tile slumping as a result of overheating. Additionally, the tiles have presented installation difficulties as well as problems with meeting step (differences in height between adjacent tiles) and gap (space between adjacent tiles) specifications. As a solution to these anomalies, the RCC chin panel assembly was designed and installed as a direct replacement for the RSI tiles located in this area (fig. 16). The Orbiter forward fuselage structures were strengthened and stiffened by the addition of new attach fittings. For the chin panel installation, these structural modifications significantly reduced the installation difficulties associated with RSI tiles.

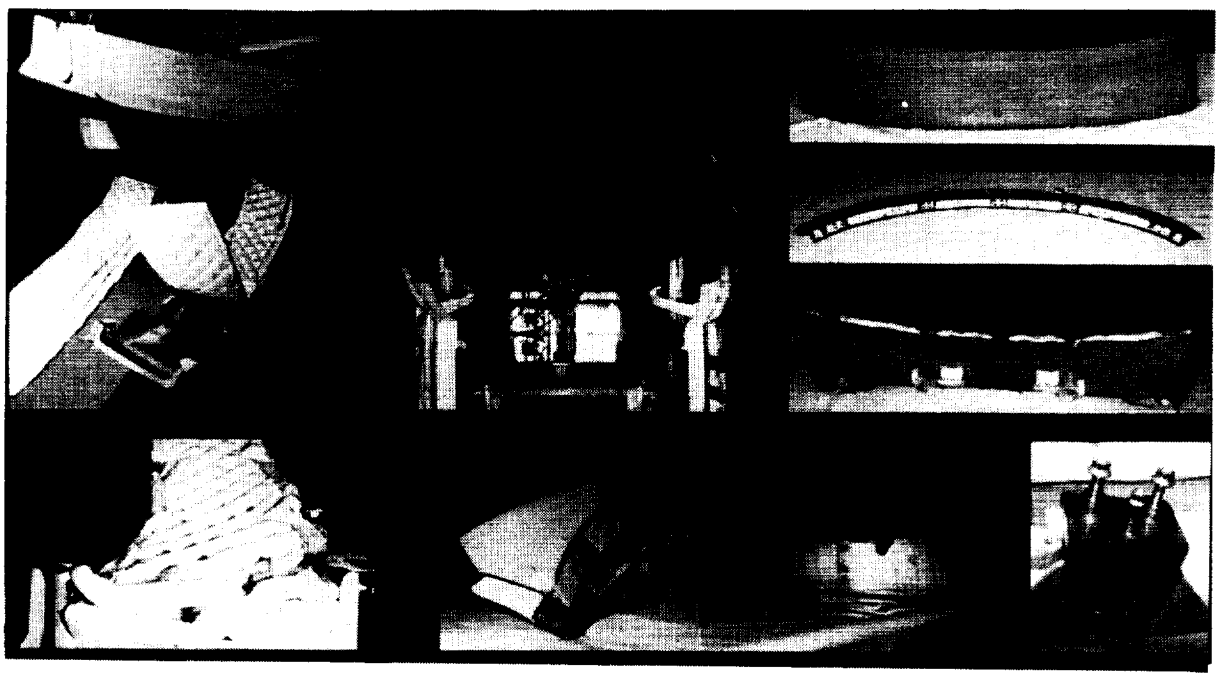

Figure 16. Orbiter RCC chin panel.

Flight performance of the chin panel has been outstanding; however, thermoelastic analyses of the flange areas have revealed higher values of thermally induced stress than originally estimated. The flange area of the chin panel was designed to minimize thermal stress (fig. 17). The low thermoelastic margins of safety (down to zero) are evaluated on flight-to-flight basis to assure chin panel acceptability.

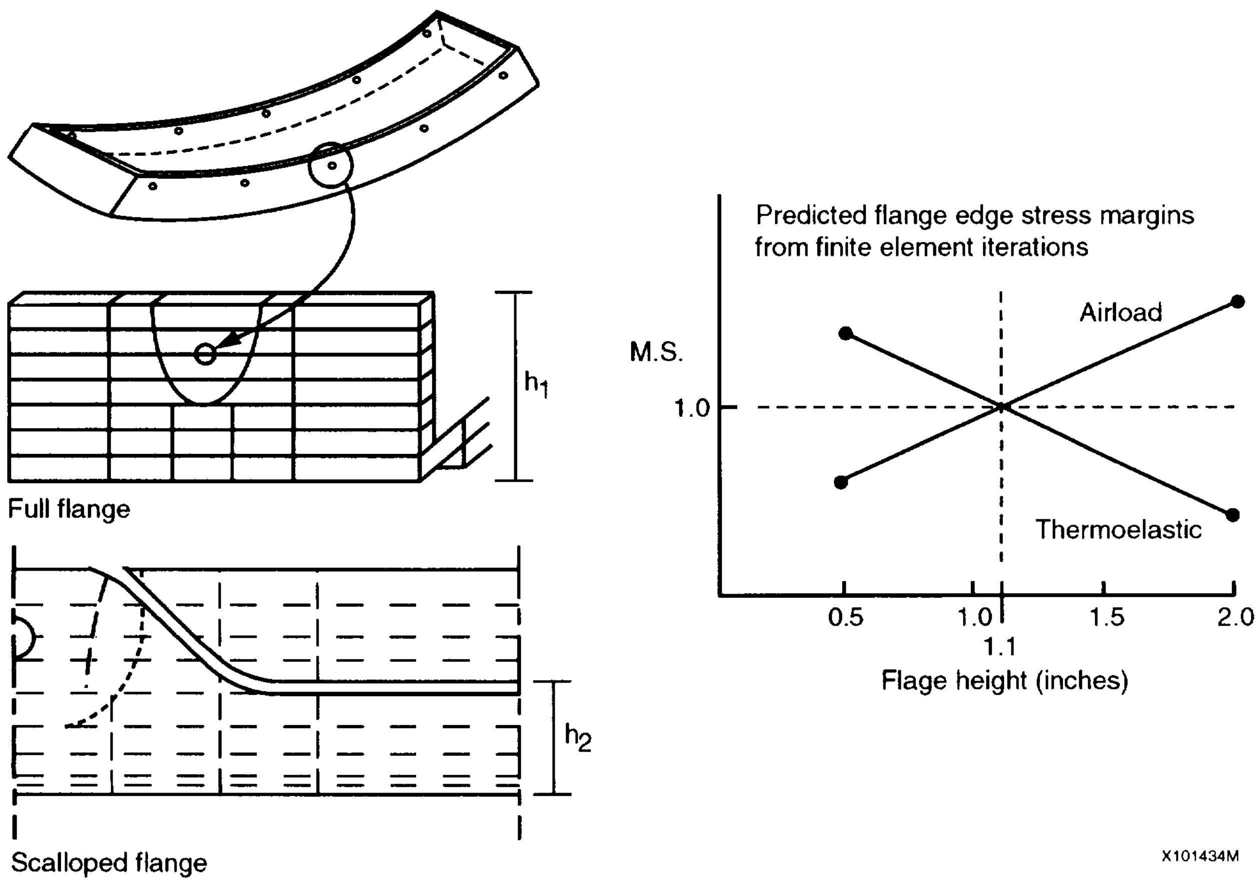

Figure 17. Chin panel flange height determination.

The reusable, oxidation protected RCC has been successfully flown on forty-three Space Shuttle Orbiter flights. The multimission life of the RCC components has been established through extensive thermal (plasma arc and radiant) and structural component tests. The RCC was originally developed to have nominal multimission capability (i.e., no surface recession) with a maximum temperature of 2800°F. However, Orbiter abort conditions can result in RCC temperatures significantly higher (>3000°F) than the multimission design value. Accordingly, an over-temperature test (3000-3400°F) program was conducted to develop surface recession correlations and establish single mission limit temperature for the RCC material. A comparison with available passive/active oxidation data in the literature for Si-O-C/Si-O-N systems, indicates that oxidation protected RCC remains passive for temperatures of 3250-3300°F (fig. 18).

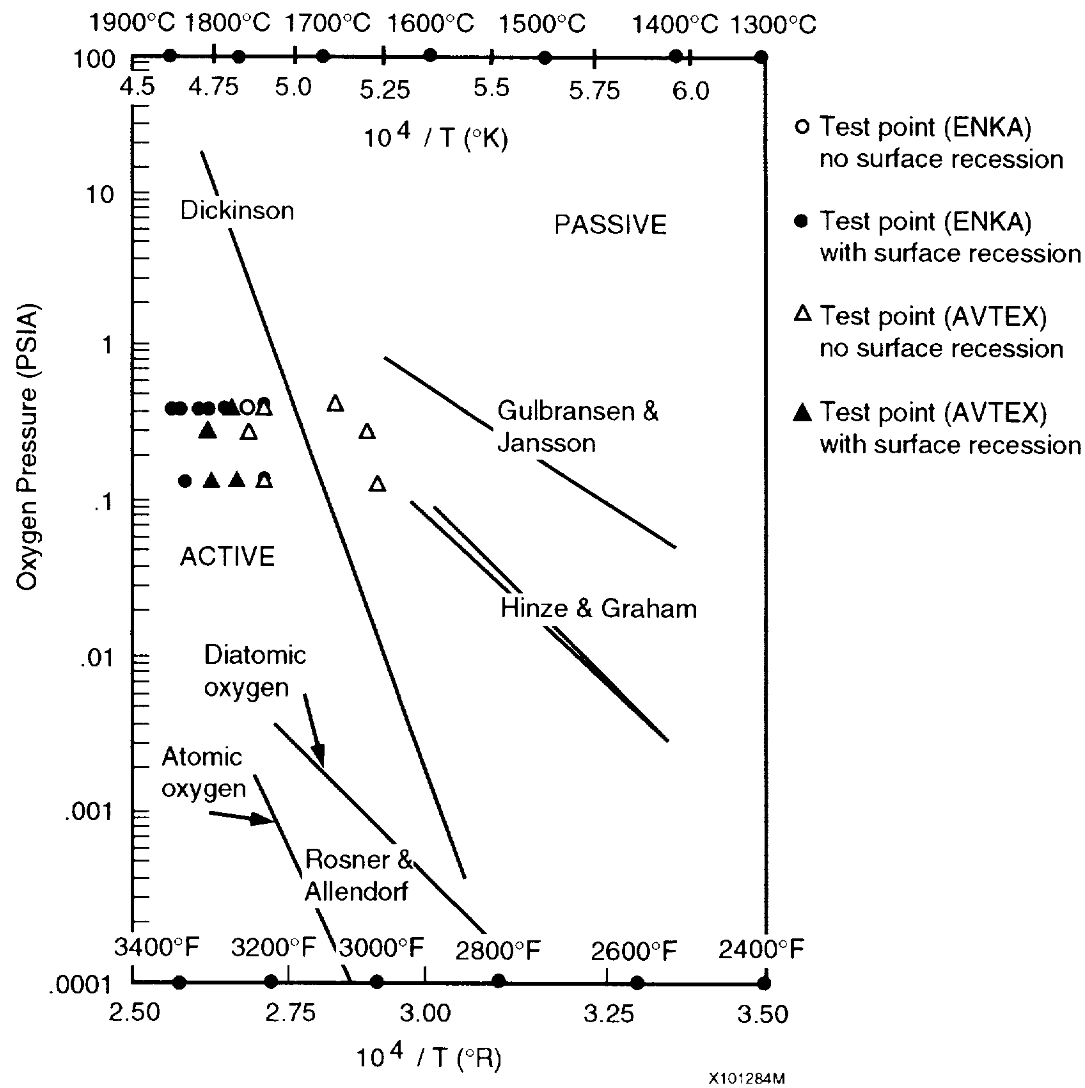

Figure 18. Active-pressure transition oxygen pressures comparisons with test conditions.

The RCC over-temperature test data has been used to increase the Orbiter ranging capability to ensure safety of flight for both nominal and off-nominal (abort) entries. A typical nominal and abort trajectory are shown on an active/passive oxidation plot (fig. 19). A nominal Earth entry is always passive but an abort condition does result in active oxidation during the entry. The time spent in the active oxidation regime is critical in assessing a potential system failure.

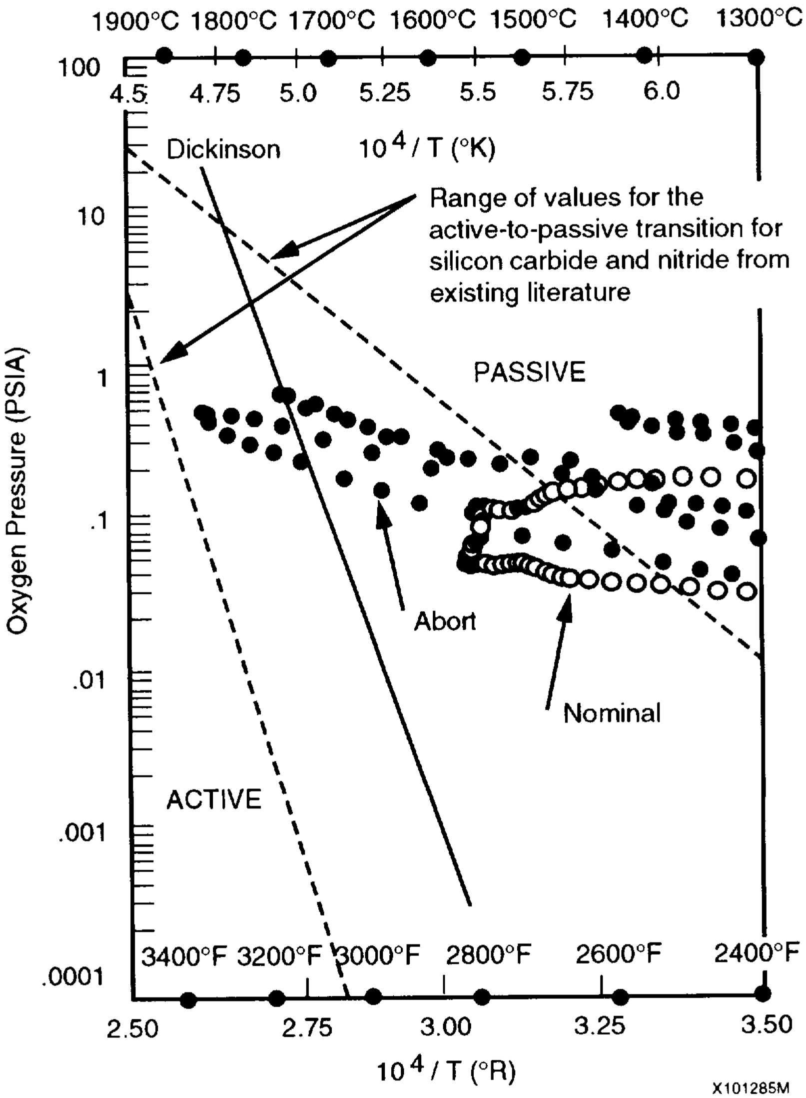

Figure 19. Active-passive transition oxygen pressures comparisons with flight conditions.

The design goal for a non-ablating, flight-certified material for the Aeroassist Flight Experiment (AFE) aerobrake TPS was accomplished by selecting an RSI material compatible with the thermal environment for a single mission use. Three rigid, reusable surface insulation materials, which were flight certified for the Space Shuttle Orbiter TPS, were considered:

LI-900/LI-2200 materials, which are basically 95% pure silica with densities of 9 lb/ft^3 and 22 lb/ft^3, respectively, and

FRCI-12, a fibrous refractory composite insulation with a density of 12 lb/ft^3.

The aerobrake heating/temperature distribution required stability at higher temperature in the stagnation region than in the other areas (2900°F). Therefore, the LI-2200 material was selected based on its shrinkage characteristics and the requirement to maintain dimensional control (fig. 20). FRCI-12 was used as the TPS material in the remaining areas.

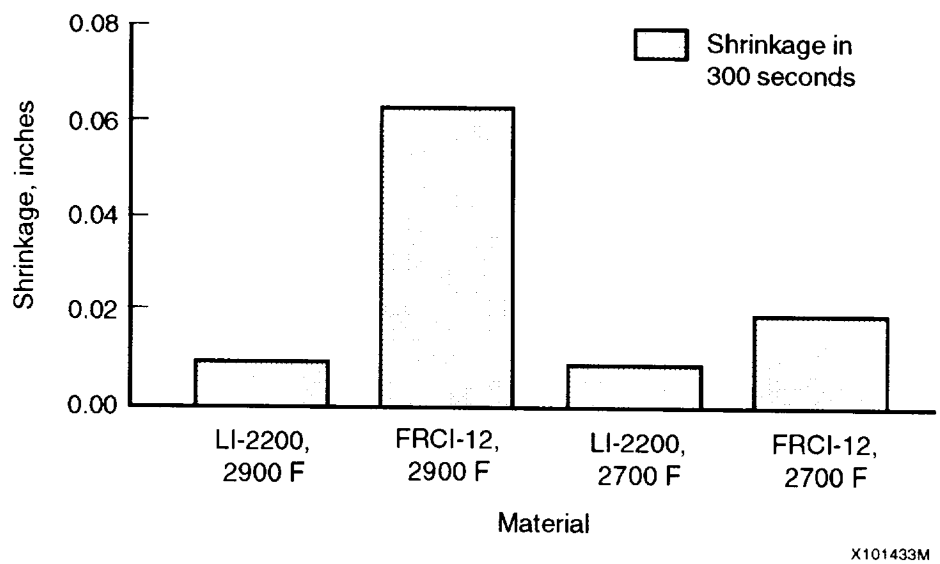

Figure 20. Over temperature RSI shrinkage evaluation.

AEROBRAKE TILE INSTALLATION

The aerobrake tiles are installed using the process developed for the Space Shuttle Orbiter (fig. 21). To isolate the tiles from stress induced by structure deflection or temperature-induced structural expansion, the tiles are bonded to a SIP, which is then bonded to the aerobrake skin. The SIP is a 0.16-inch Nomex nylon felt material. The bonding is performed using Room Temperature Vulcanizing adhesive #560 (RTV-560). The gaps between the tiles are filled with the Ceramic Ames Gap Filler (CAGF) to prevent plasma flow from heating the inner-tile gap. These gap fillers are composed of several layers of Nextel (alumina silicate) cloth (AB312) impregnated with a ceramic coating. Several layers are bonded to the bottom sidewall of one neighboring tile with a ceramic adhesive. Gap filler installation and the use of a full footprint SIP are modifications to the Orbiter tile installation.

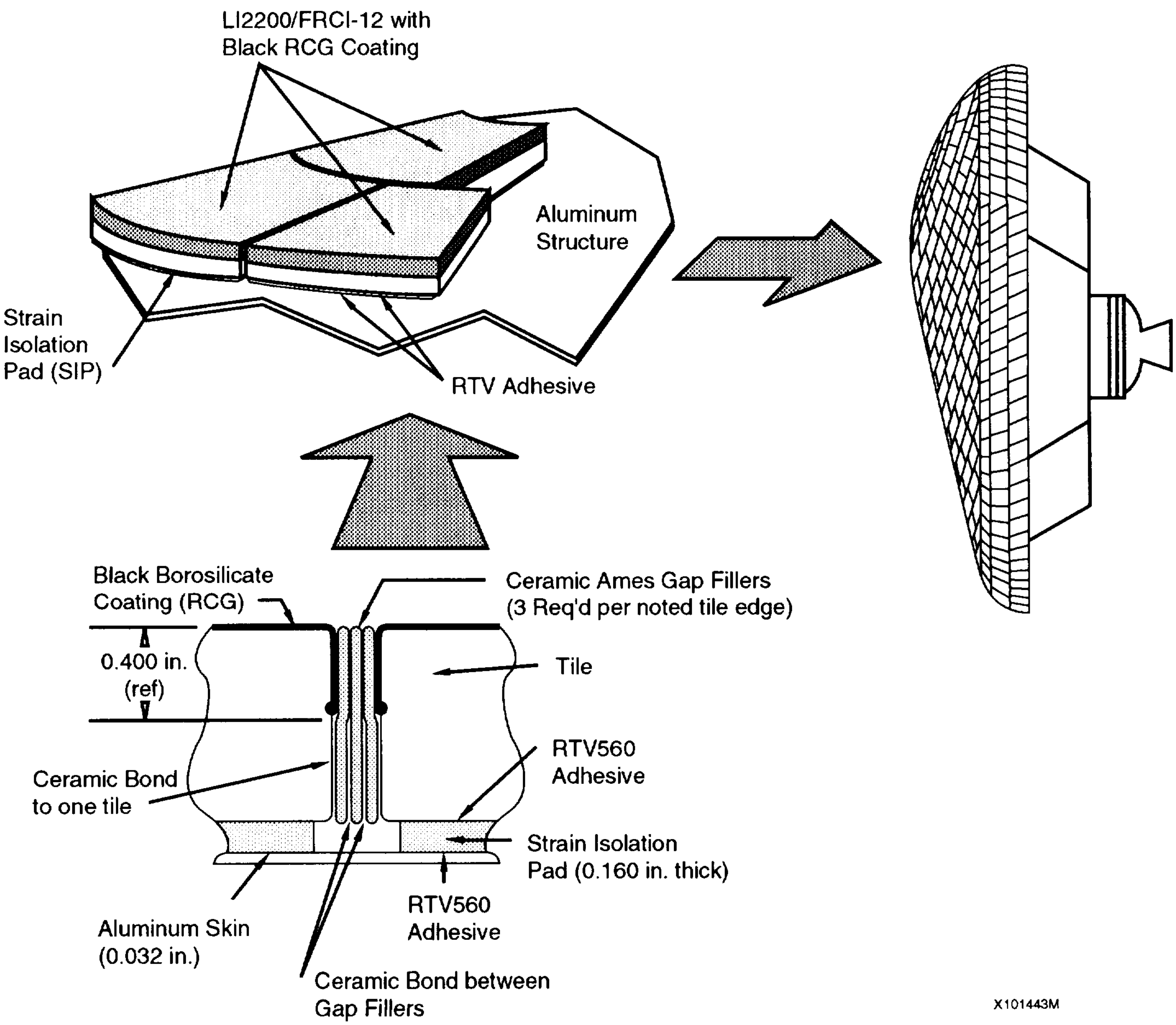

Figure 21. Aerobrake TPS installation.

AEROBRAKE TILE CONFIGURATION/MANUFACTURING

The LI-2200 tiles on the ellipsoid were made larger than baseline Space Shuttle Orbiter tiles (6-inch by 6-inch), due to the more rigid structure of the ellipsoid and the higher strength of the LI2200 material. In the cone and skirt area, the FRCI-12 tiles were sized smaller, as much larger skin deflections are expected in those area (fig. 22).

Numerically controlled machining processes were used to manufacture AFE tiles, as was done for the Orbiter. The Calma CAD system was utilized to automate the design process and facilitate efficient transfer of data to the N-C machining process. This resulted in cost and time savings by reducing the N-C programming efforts and the number of close-out tiles needed, and by eliminating the need to sand the inner moldline of each individual tile during installation.

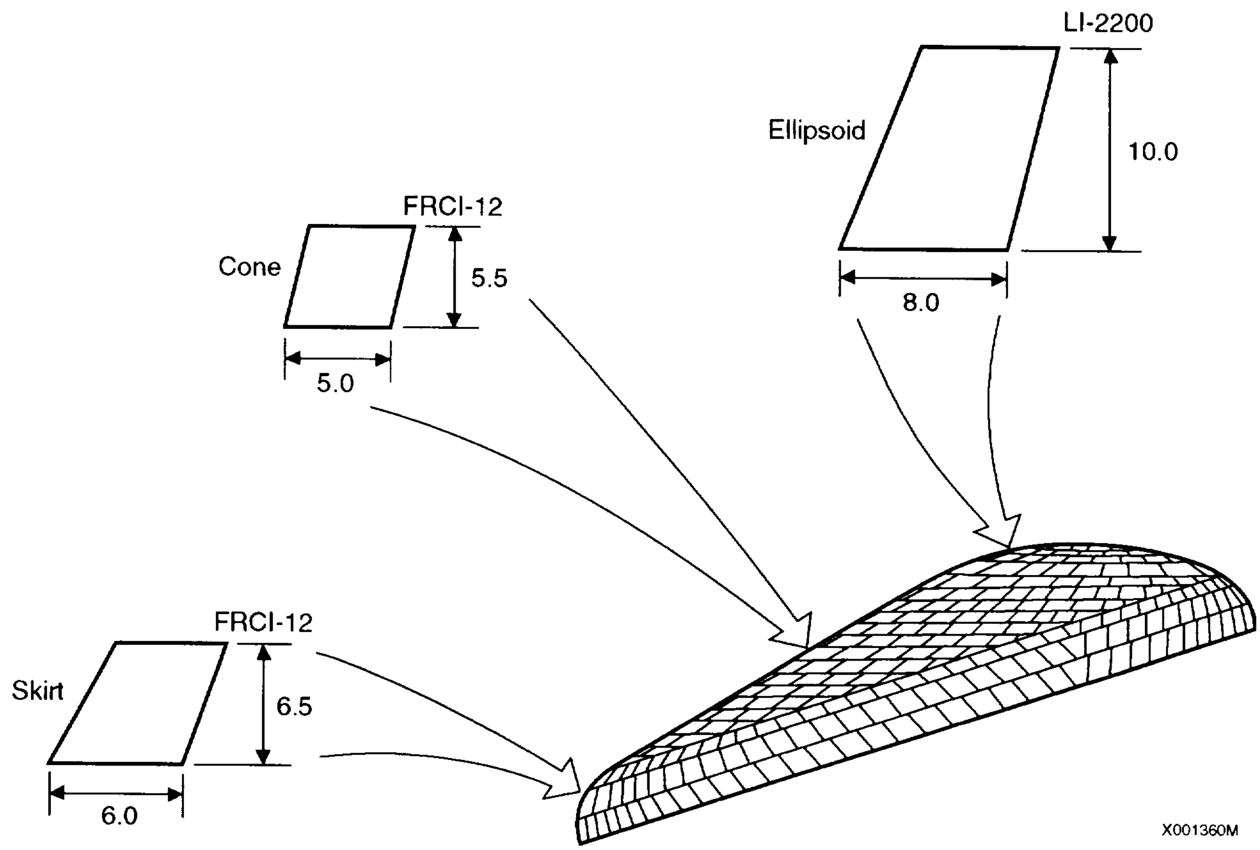

Figure 22. Typical tile sizes and materials.

TPS DESIGN FOR AEROBRAKING AT EARTH AND MARS

Thermal protection systems are being designed for advanced vehicle configuration and future missions using state-of-the-art materials for a wide range of entry conditions. The performance of an ablation material (5026-H/CG) applied to a 40-foot aerobrake (AFE configuration) that performs two aerocaptures (Mars and Earth) without refurbishment was analyzed.

The ablation analysis was performed in two steps: surface recession and mass loss were first predicted for Mars entry, then these values were used as initial conditions for the Earth aerocapture.

The results of this analysis suggest that optimal ablator thickness can be determined such that more than one successful entry can be made without refurbishment. Critical sizing of the ablator was established from the thermal response for the Earth return. Material degradation (density ratio) can be used to assess thermal/structural performance (fig. 23).

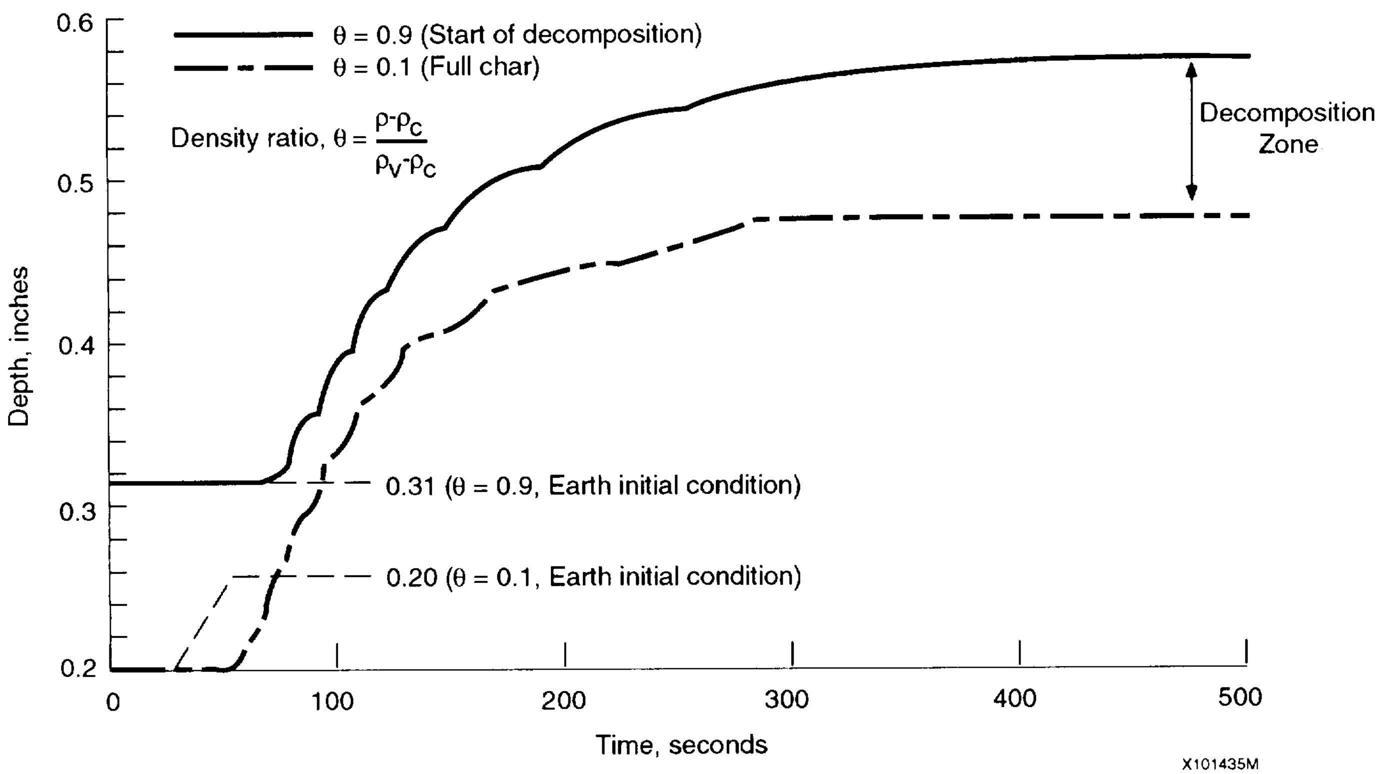

Figure 23. Earth aerocapture for the 40 ft. AFE- 0.9 and 0.1 density ratio depths at the stagnation point.

TPS DESIGN FOR AEROBRAKING WEIGHT PENALTY

TPS assessments for future vehicle and missions can be made using TPS weight penalty factors. A TPS penalty factor can be defined as:

$$\eta_t = \frac{\text{TPS Weight}}{\text{Total Vehicle Weight}}$$

$$\eta_s = \frac{\text{Structural Weight}}{\text{Total Vehicle Weight}}$$

$$\eta_{ts} = \eta_t + \eta_s$$

Figure 24 a, b shows the relationship between η_s and η_t for several vehicle configurations used for an aerocapture at Earth and Mars. These results indicate that an η_{ts} of 15-20 percent is possible utilizing aerobraking, which results in a predicted 50-80 percent increase in payload over an all-propulsive design.

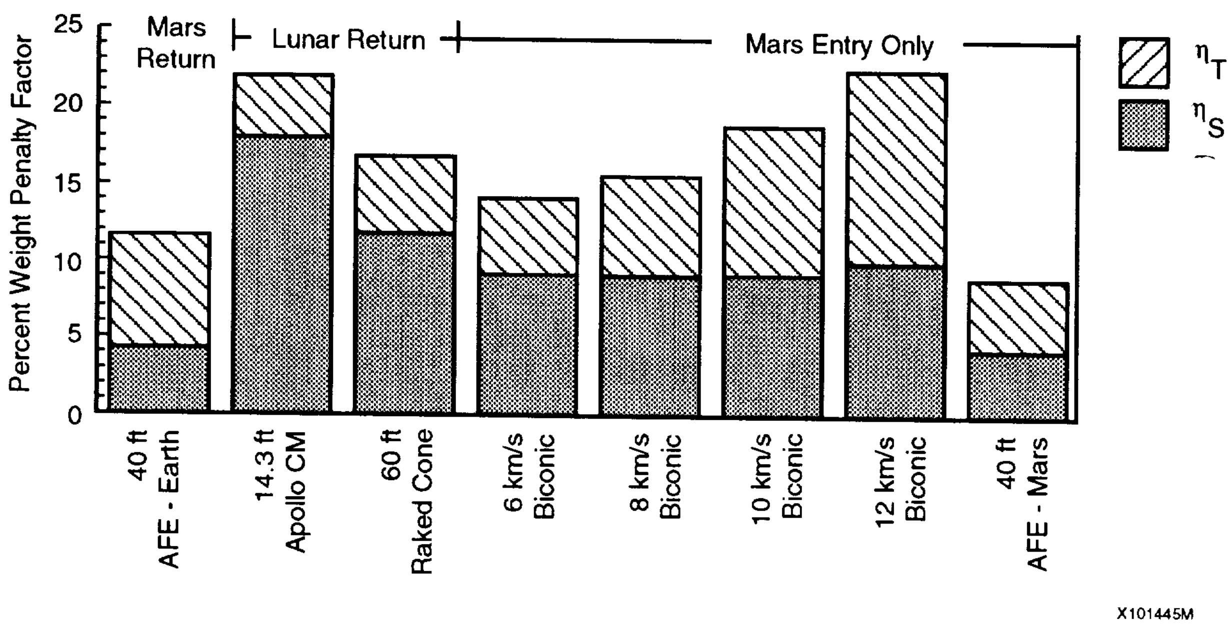

Figure 24a. Weight penalty factors for TPS/structure weights.

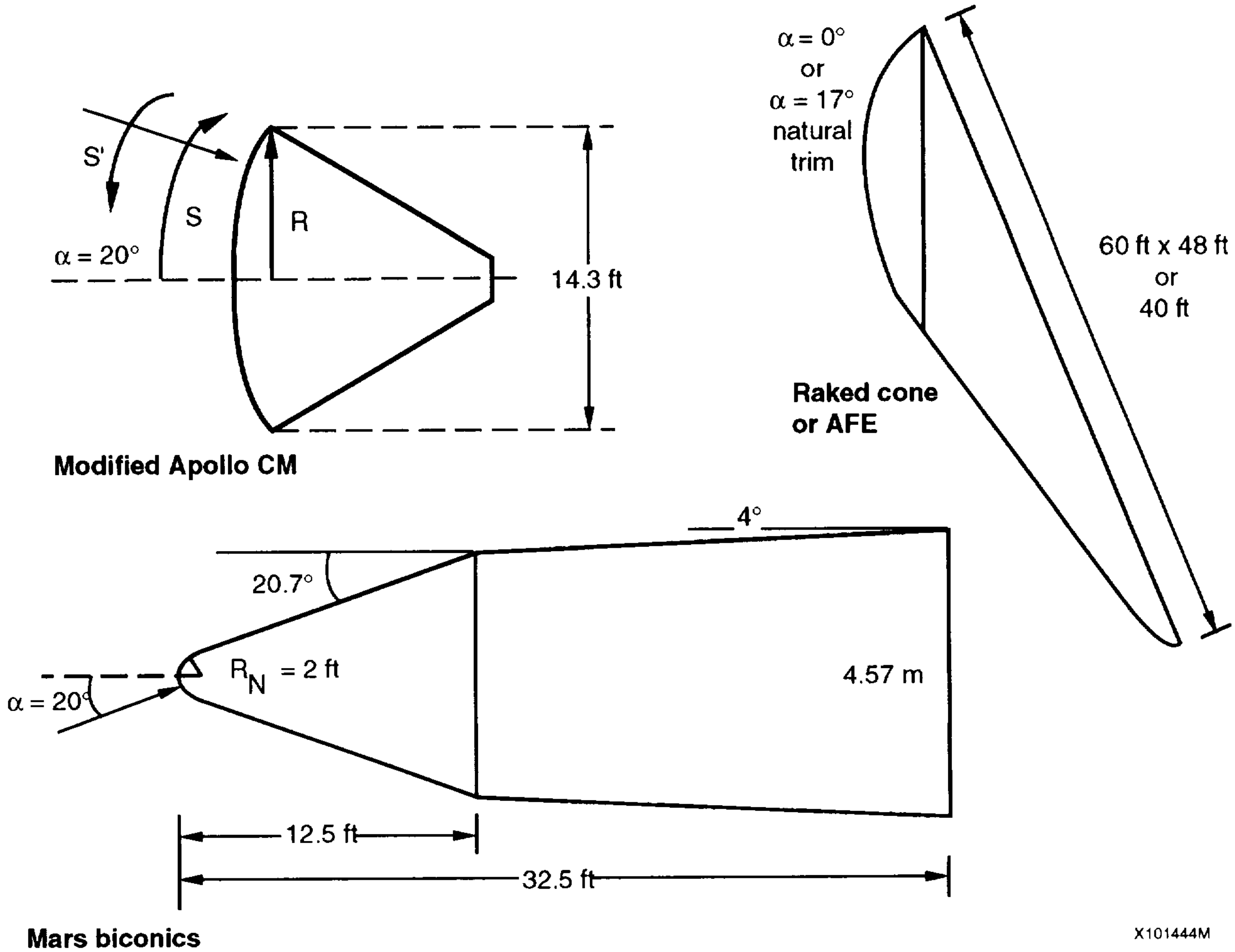

Figure 24b. Earth/Mars aerocapture vehicles.

SUMMARY

- Significant advances have been made in the design, fabrication, and certification of TPS on manned entry vehicles (Mercury through Shuttle Orbiter)
- Shuttle experience has identified some key design and operational issues
- State-of-the-art ceramic insulation materials developed in the 1970s for the Space Shuttle Orbiter have been used in the initial designs of aerobrakes
- This TPS material experience has identified the need to develop a technology base from which a new class of higher temperature materials will emerge for advanced space transportation vehicles.